GIG Research Institute

JOURNAL OF SUSTAINABLE MINING

Volume 22 | Issue 1 Article 5

2023

Research on vibration-based early diagnostic system for excavator motor bearing using 1-D CNN

Author(s) ORCID Identifier:
Dorjsuren Yandagsuren: 0000-0002-5307-931X
Tatsuki Kurauchi: 0000-0002-6409-331X
Hisatoshi Toriya: 0000-0001-6753-5681
Hajime Ikeda: 0000-0002-0863-5583
Tsuyoshi Adachi: 0000-0003-0556-7527
Youhei Kawamura: 0000-0003-4103-762X

Research on vibration-based early diagnostic system for excavator motor bearing using 1-D CNN

Abstract

In mining, super-large machines such as rope excavators are used to perform the main mining operations. A rope excavator is equipped with motors that drive mechanisms. Motors are easily damaged as a result of harsh mining conditions. Bearings are important parts in a motor; bearing failure accounts for approximately half of all motor failures. Failure reduces work efficiency and increases maintenance costs. In practice, reactive, preventive, and predictive maintenance are used to minimize failures. Predictive maintenance can prevent failures and is more effective than other maintenance. For effective predictive maintenance, a good diagnosis is required to accurately determine motor-bearing health. In this study, vibration-based diagnosis and a one-dimensional convolutional neural network (1-D CNN) were used to evaluate bearing deterioration levels. The system allows for early diagnosis of bearing failures. Normal and failure-bearing vibrations were measured. Spectral and wavelet analyses were performed to determine the normal and failure vibration features. The measured signals were used to generate new data to represent bearing deterioration in increments of 10%. A reliable diagnosis system was proposed. The proposed system could determine bearing health deterioration at eleven levels with considerable accuracy. Moreover, a new data mixing method was applied.

Keywords

bearing diagnosis, electric motor, vibration analysis, signal processing, 1-D CNN

Authors

Dorjsuren Yandagsuren, Tatsuki Kurauchi, Hisatoshi Toriya, Hajime Ikeda, Tsuyoshi Adachi, and Youhei Kawamura

Research on vibration-based early diagnostic system for excavator motor bearing using 1-D CNN

Dorjsuren Yandagsuren [a,c,*], Tatsuki Kurauchi [a], Hisatoshi Toriya [a], Hajime Ikeda [a], Tsuyoshi Adachi [a], Youhei Kawamura [b]

[a] Akita University, Faculty of International Resource Sciences, Japan
[b] Hokkaido University, Division of Sustainable Resources Engineering, Japan
[c] Mongolian University of Science and Technology, School of Geology and Mining, Mongolia

Abstract

In mining, super-large machines such as rope excavators are used to perform the main mining operations. A rope excavator is equipped with motors that drive mechanisms. Motors are easily damaged as a result of harsh mining conditions. Bearings are important parts in a motor; bearing failure accounts for approximately half of all motor failures. Failure reduces work efficiency and increases maintenance costs. In practice, reactive, preventive, and predictive maintenance are used to minimize failures. Predictive maintenance can prevent failures and is more effective than other maintenance. For effective predictive maintenance, a good diagnosis is required to accurately determine motor-bearing health. In this study, vibration-based diagnosis and a one-dimensional convolutional neural network (1-D CNN) were used to evaluate bearing deterioration levels. The system allows for early diagnosis of bearing failures. Normal and failure-bearing vibrations were measured. Spectral and wavelet analyses were performed to determine the normal and failure vibration features. The measured signals were used to generate new data to represent bearing deterioration in increments of 10%. A reliable diagnosis system was proposed. The proposed system could determine bearing health deterioration at eleven levels with considerable accuracy. Moreover, a new data mixing method was applied.

Keywords: bearing diagnosis, electric motor, vibration analysis, signal processing, 1-D CNN

1. Introduction

Different types of excavators are used in mining, including shovels, draglines, and hydraulic excavators. They are equipped with motors to operate hoists, swings, crowds, and propelling mechanisms. This study considers the bearing diagnostic of the electric motor in the crowd mechanism of the mining shovel in the Baganuur mine (EKG-5a). The Baganuur mine was established in 1978 and is one of the largest coal suppliers for Mongolian power plants [1]. A strip mining method is used in the mine. The mine contains brown coal and has an area of 31.6 km^2 [1]. The EKG-5a excavator is the primary machinery used for coal excavation.

Electric motors are an important component of rope shovels and are often damaged in harsh mining environments. Failures can occur in the shaft coupling, rotor winding, stator winding, and bearings. Over 40% of total motor failures are related to the bearings [2–6]. One study reported that bearing failure accounts for 51% of overall motor failure [7]. Different types of bearing failure can occur, including inner ring faults, outer ring faults, ball faults, and deterioration. The main causes of motor bearing failure are insufficient or excessive lubrication, overheating, long-term operation, overload, greasing type, incorrect installation, pollution of bearing lubrication, and working conditions. Pollution of the lubrication material leads to rapid deterioration of the bearing and reduces the factory-normalized lifetime of the bearing. If machines continue to operate with failed bearings, the work efficiency decreases, and failure is transmitted to other joint parts, producing other machine faults.

Received 9 February 2022; revised 9 November 2022; accepted 2 December 2022.
Available online 11 January 2023

* Corresponding author at: Akita University, Faculty of International Resource Sciences, Japan.
E-mail address: dorjsuren@must.edu.mn (D. Yandagsuren).

https://doi.org/10.46873/2300-3960.1377

Thus, bearing failures must be detected quickly. Vibration measurement is commonly used to diagnose the health of rotating machines such as motors, rotors, gearboxes, drill bits, and bearings [6,8–27]. Researchers have used vibration diagnosis to detect bearing faults [6,8–22]. Most have focused on the inner ring, outer ring, and ball faults in motor bearings [6,8–11,13–22]. One study [12] examined four levels of bearing health monitoring (healthy, early fault, moderate fault, and severe fault) based on vibration diagnostics. In practice, considerable bearing deterioration occurs, requiring more accurate monitoring. Hence, eleven levels of motor-bearing health deterioration were considered in this study, which is deemed sufficient for an in-depth analysis of bearing failure.

In the past two decades, the development of information and communication technology (ICT) has been a global trend. Deep learning, a sector of machine learning, has been developed since 1991 [28]. Some industrial sectors are using deep learning to reduce costs and increase productivity. Many researchers have used deep neural networks and vibration data from rotating machines; more than half of them used a CNN model [6,9,11,12,14–19,21,22,24–27]. In a study [15] comparing CNNs against other deep learning models, it was further concluded that CNNs are better than other deep learning models. This advantage stems from its compact structural architecture, cost-efficiency and practicality (real-time hardware implementation). Hence, the CNN output was greater than other models in the study. In another paper [16], CNNs were favoured for their low computational load and lower risk of overfitting, which greatly improves the accuracy and efficiency of pattern recognition. Furthermore, the 1-D CNN possess the highest accuracy (99.9%) compared with LSTM (Long-Short Term Memory), Support Vector Machine (SVM), k-Nearest Neighbors (kNN), Multilayer Perceptron (MLP) and Random Forest in their study of vibration-based bearing fault recognition. Therefore, it can be said that CNNs are considerably effective for data classification, and can be used in one-dimensional (1-D), two-dimensional (2-D), and three-dimensional (3-D) forms. In a study by Wang et al. [17], outputs from 1-D and 2-D CNNs have been compared in bearing fault diagnosis; with the 1-D CNN outputting better results. For these reasons, a 1-D CNN deep learning algorithm is used to diagnose bearing health deterioration in our study.

In one study, a 1-D CNN was used to classify drill bit failure based on the acceleration waveform [27]; in another study, a deep neural network was used to distinguish bearing and gearbox failure based on vibration and acoustic data [10].

In practice, machine health monitoring, particularly bearing and gearbox diagnosis systems based on vibration and machine learning, are faced with a lack of training data. To solve this problem, a plethora of research works [38–42] have employed various kinds of generative adversarial networks (GANs). In these studies, random noise, standard noise and/or fake samples (distributed noise) were used to generate data. More precisely, studies by Zhao et al. [41] and Guo et al. [42] proposed GANs to generate data for the evaluation of inner ring, outer ring and rolling element fault. Hence, this research differs from the previously stated works [38–42] in that it takes into consideration the bearing deterioration in the generation of new data.

Research by Song et al. [43] considered a retraining strategy based domain adaption network (DAN-R) on bearing fault diagnosis. DAN is usually applied to reduce the disparity between features of various domains. The aim of this research is thus to make clear differences between neighbor classes. Therefore, traditional CNNs are best suited for this task.

Many studies [44–51] have been undertaken to accurately estimate bearing health as a means to determine the remaining viability of such bearings using CNNs, artificial neural networks (ANNs) and deep neural networks (DNNs). Based on measured monitoring data, these studies demonstrated the great capabilities of these systems by employing techniques such as autoencoders, multiscale feature extraction, long-short term memory (LSTM) and health indicators (HI). On the other hand, this study differs from the above mentioned as it employs a new data generation feature-extraction method coupled with a CNN.

Bearing failure detection experiments were performed in a laboratory in some studies; typically, low-power motors were used in the experiments [8,11,15,16,18,19,21,26]. To properly estimate bearing deterioration, data should be collected from an actual system.

In practice, three maintenance strategies are generally used to mitigate failures: reactive, preventive, and predictive maintenance [29,30]. Reactive strategies are considered outdated as they entail repairing machines after a failure occurs. This method has disadvantages, such as high repair costs and significant machine productivity losses. Preventive maintenance is typically used to decrease economic losses [29,31] and is a better economic indicator than reactive maintenance, although it

Fig. 1. EKG-5a excavator.

increases repair costs. In recent years, predictive maintenance has emerged; it is the most effective maintenance method for estimating remaining useful life (RUL) and decreasing the economic losses of machines [30,31]. In a report by the US Office of Energy Efficiency and Renewable Energy, good results were achieved when predictive maintenance was used instead of reactive maintenance. Return on investment was tenfold; maintenance costs were reduced by 25–30%; breakdowns were reduced by 70–75%; downtime was reduced by 35–45%, and machine productivity was increased from 20% to 25% [30]. Researchers reported an economic improvement of 26.02% when predictive maintenance was used instead of preventive maintenance [29]. Predictive maintenance is performed on the basis of good diagnostics.

The purpose of this study is to reduce economic losses and increase the productivity of mining excavators. A predictive maintenance method must be used in the mining sector. A CNN and vibration-based bearing-health monitoring can satisfy these requirements. To this end, vibration data should be measured at an actual site. The CNN must correctly assess the motor bearing health deterioration to determine the RUL of the bearing. However, in an actual system, only normal and failed data can be clearly measured; bearing health deterioration is uncertain. Thus, new data must be generated based on the measured data to represent motor bearing health deterioration levels more accurately. For this purpose, a new data generation (mixing) method was applied in this investigation.

The CNN and vibration-based monitoring system for bearing health allow rapid and reliable detection of bearing deterioration without human intervention.

2. System design

The research object is the electric motor bearing of the EKG-5a mining excavator. The motor is model 4GPEM 55-2/1U2 (4ГПЭМ 55-2/1У2) and is used in the EKG-5a mining excavator as a generator for the crowd mechanism. The bearing model is USSR-3-18GPZ-314 (USSR-3-18ГП3-314), produced in the Russian Federation. The EKG-5a excavator used in the Baganuur mine is shown in Fig. 1. Our research process is shown in Fig. 2.

This study consists of three main parts: data collection, signal analysis (spectral analysis), and CNN training. Some additional areas of study related to the bearing health monitoring requirements were necessary. Figure 2 shows a simplified research overview. However, the purpose of this research is to evaluate bearing deterioration levels accurately using CNNs in order to implement predictive maintenance. Therefore, detailed analytical methods of the

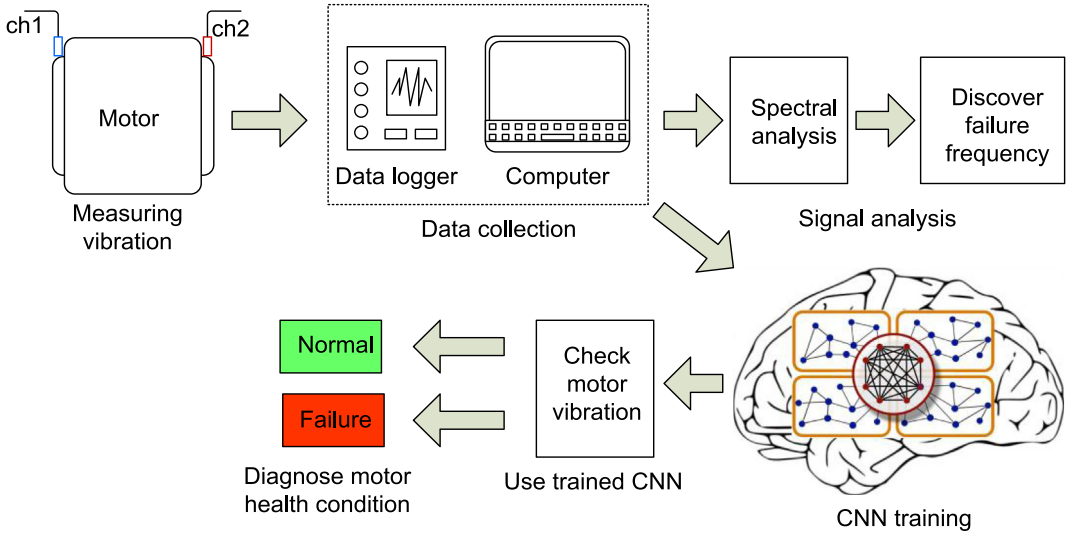

Fig. 2. Research process [37].

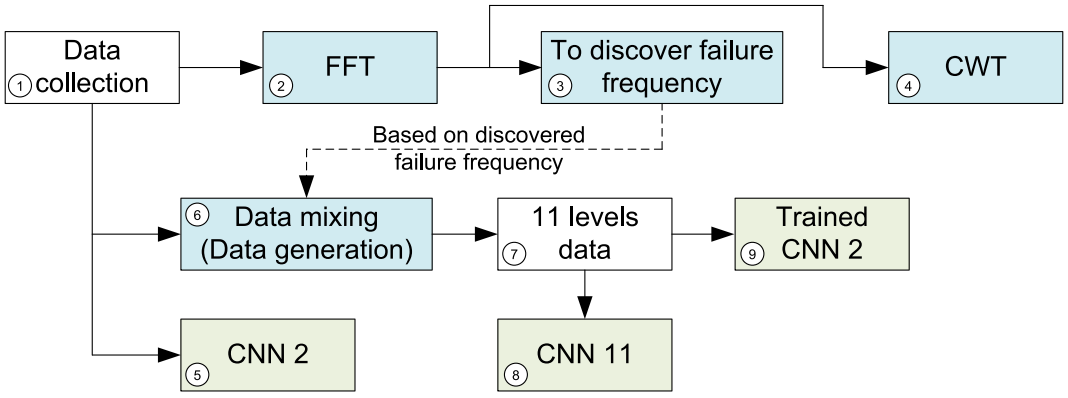

Fig. 3. Flow chart of analytical methods.

research are introduced in Fig. 3, which consists of nine explicitly described parts. Normal and failure vibrations of motor bearings are measured, and this stage is called data collection (1). Fast Fourier Transformation (FFT) (2) analyzes are done on the measured vibrations to discover failure frequency (3). After FFT, the features of bearing failure are extracted. Continuous Wavelet Transform (CWT) is performed after FFT to confirm the results of FFT (4). A "CNN with 2 classifications" (CNN 2) is trained using measured vibrations (5). Data mixing/generation is performed based on discovered failure frequency of bearings using measured vibrations (Normal and Failure) to accurately evaluate bearing deterioration levels (6). Mixed data should represent bearing deterioration from normal to failure in increments of 10%, which consists of eleven data levels (Normal, 10% Failure, 20% Failure, 30% Failure, 40% Failure, 50% Failure, 60% Failure, 70% Failure, 80% Failure, 90% Failure, and total Failure) (7).

A "CNN with 11 classifications" (CNN 11) is trained using eleven levels of data (8). Consequently, bearing deterioration can be evaluated at 10% increments. In practice, technical and economic requirements are assessed, and these include price, simplicity in application and compactness of equipment used in diagnostic systems of machines. Hence, a trained "CNN with 2 classifications" should be applied instead of the "CNN model with 11 classifications" (9). Based on these considerations, the "CNN with 2 classifications" is used to evaluate the RUL of bearings using eleven data classes. Therefore, this system should be inspected for being able to use in practice.

2.1. Experimental setup

Data were collected from a maintenance facility in the Baganuur mine. The data collection process is shown in Fig. 4. A TEAC piezoelectric acceleration sensor and a Keyence NR-500 data logger were used for data collection.

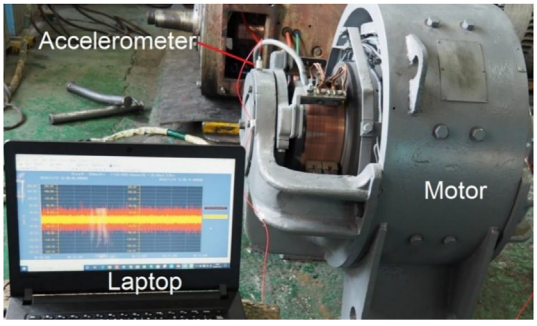

Fig. 4. Data collection at mine site [37].

An accelerometer was mounted on the bearing house of the motor, as shown in Fig. 4. The accelerometer was connected to a channel of the data logger. The bearing failure vibrations were collected using a deteriorated bearing. The deteriorated bearing was replaced with a new bearing, and the vibrations of the normal bearing were collected. The experimental specifications and setup are presented in Table 1.

Figures 5 and 6 show a normal bearing structure and a deteriorated bearing.

The working conditions cause the rolling elements of the bearing to deteriorate, resulting in excessive vibration. The deterioration is shown in Fig. 6.

Table 1. Data collection specifications [37].

Specification	Unit	Value
Sampling frequency	kHz	100
Sampling period	μs (microsecond)	10
Sampling duration	s	60
Sampling count	–	60 (Normal 30, Failure 30)
Motor rotation speed	rpm	1200

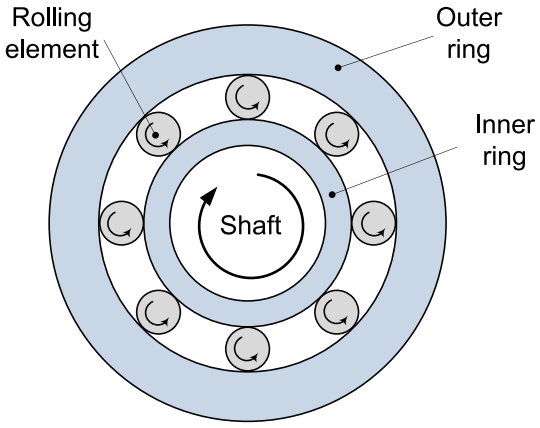

Fig. 5. Motor bearing structure [37].

2.2. Waveform

The measured vibrations are shown in Fig. 7.

The waveforms in Fig. 7 are similar, except at times in amplitude; it is difficult to distinguish the difference between them. Thus, other signal processing techniques are required.

2.3. Frequency analysis

2.3.1. Fast Fourier Transform

In practice, every movement causes vibrations, and all vibrations are combined. This makes it difficult to distinguish which part(s) of vibrations were generated by bearing failure. Also, an accelerometer collects combined vibrations. Hence, the Fast Fourier Transform (FFT) is usually used for frequency analysis to allow the critical frequency to be easily distinguished. Time-domain data are converted into the frequency domain using FFT, also known as spectral analysis. The dominant frequencies of the vibration data can be easily determined, confirming the difference between normal and failure-bearing conditions. FFT analysis was used to examine the normal and failure data of bearing, as shown in Fig. 8.

Fig. 6. Bearing failure (deterioration) [37].

After FFT analysis in Fig. 8, the dominant frequency range of bearing failure was observed between 400 and 450 Hz, which is failure frequency, as indicated in the red box. If the bearing failure level increases, the amplitude of failure vibration is elevated when speed is constant. In this case, the motor speed was constant at 1200 rpm when vibration measurements were performed. Therefore, motor bearing failure amplitudes of vibrations increased linearly in a frequency range between 400 and 450 Hz. Another frequency range from 800 to 1100 Hz was shifted to the left (indicated by the blue box). Using FFT, the difference between normal and failure is made clear, hence, the development of an automatic diagnostic system is made possible.

2.3.2. Wavelet analysis

In FFT analysis, time information is lost, and the data are visualized as the amplitude of the sine or cosine functions. Thus, wavelet analysis is required for signal processing. Wavelet analysis simultaneously provides time, frequency, and amplitude information, and is sometimes referred to as time-frequency analysis. A continuous wavelet transform (CWT) was used to analyze the data. The CWT equation is presented in Eq. (1) [32].

$$W(a,b) = \int_{-\infty}^{\infty} \frac{1}{\sqrt{a}} s(t)\psi\left(\frac{t-b}{a}\right)dt \tag{1}$$

where a is the time interval corresponding to the bandpass filter ($a>0$); b is the translation of the wavelet and provides for time localization; t is time; $\psi(t)$ is the mother function; $s(t)$ is the signal; $W(a,b)$ is the continuous wavelet transform.

The wavelet analysis results are shown in Fig. 9, which shows the normal and failure conditions for bearing health.

The motor speed was 1200 rpm during the experiments; 0.05 s represents one rotation of the motor. Different wavelet types, including MexHat, Morlet, and DGauss can be used in wavelet analysis. The MexHat (Mexican hat) wavelet was used in our analysis; it is a commonly used wavelet type and is a smooth continuous function. The vertical axis represents the frequency (Hz), and the horizontal axis represents time (s), as shown in Fig. 9. The amplitude of the acceleration corresponding to the frequency is expressed by the color brightness.

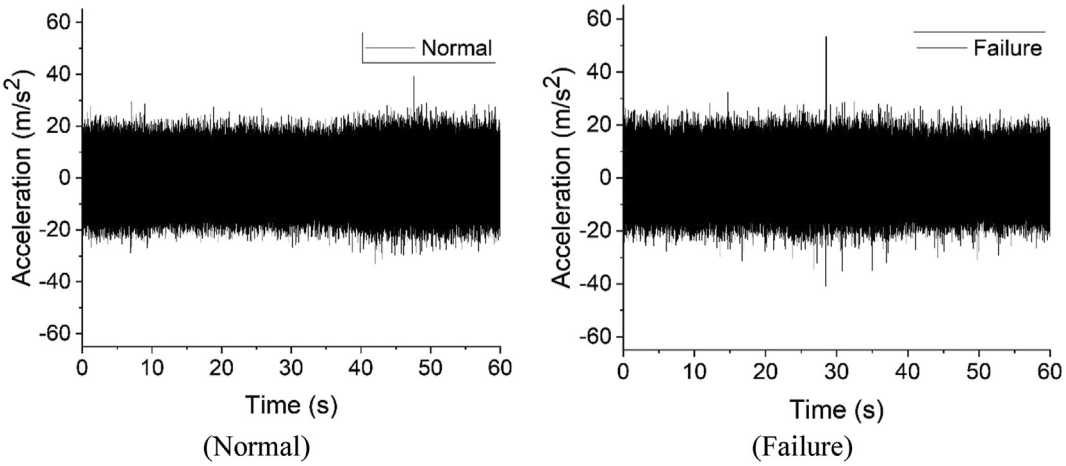

Fig. 7. Bearing vibration waveforms.

A light color indicates a large amplitude; a dark color indicates a small amplitude. CWT allows for the confirmation of FFT and the determination of critical frequencies belonging to specific time zones. Figure 9 shows that the bearing failure amplitudes (B. Failure) were higher than normal (A. Failure) at a frequency range between 400 and 450 Hz, except for time zones between 0.036 and 0.039 s. By way of explanation, bearing deterioration generates high amplitude vibrations per one rotation of the motor.

3. Convolutional neural network

Convolutional neural networks (CNNs) are powerful artificial neural networks suitable for classification. They have provided excellent results in image and speech recognition and have been used by researchers [33,34]. A CNN consists of many neural network layers, including input, convolution, batch normalization, max pooling, dropout, fully connected, and SoftMax layers. These layers determine the input data features used for classification.

The convolution layer is a fundamental CNN component used for feature extraction [35]. It is usually joined with a pooling layer and an activation function. A pooling layer is commonly used after the convolution layer for matrix dimension reduction and data feature extraction [14]. Different types of pooling layers, such as max pooling and mean pooling layers, are used in CNNs; max-pooling layers are the most common [14,35]. Activation functions, including sigmoid, tanh, ReLU, Leaky ReLU, Parametrized ReLU, ELU, Swish, and SoftMax, are used in artificial neural networks as binary step functions [36], which must be nonlinear. ReLU is most commonly used.

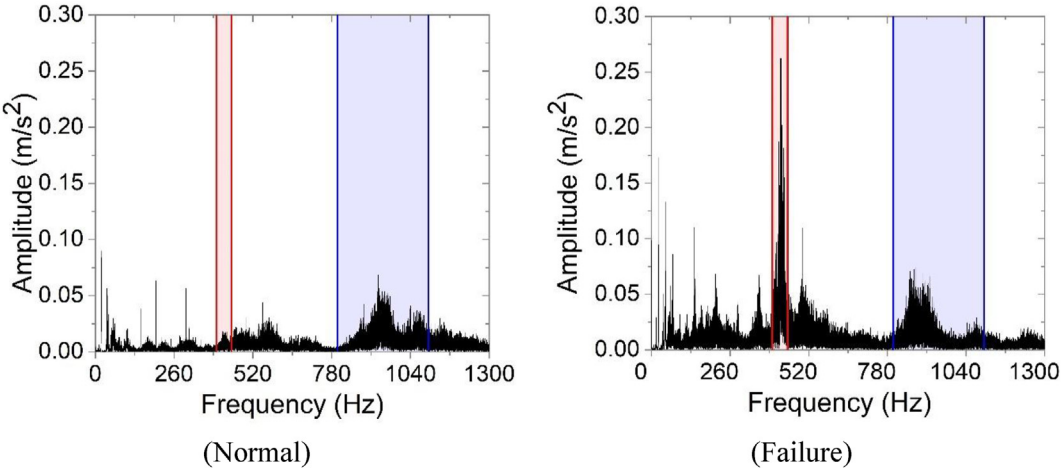

Fig. 8. FFT analysis results.

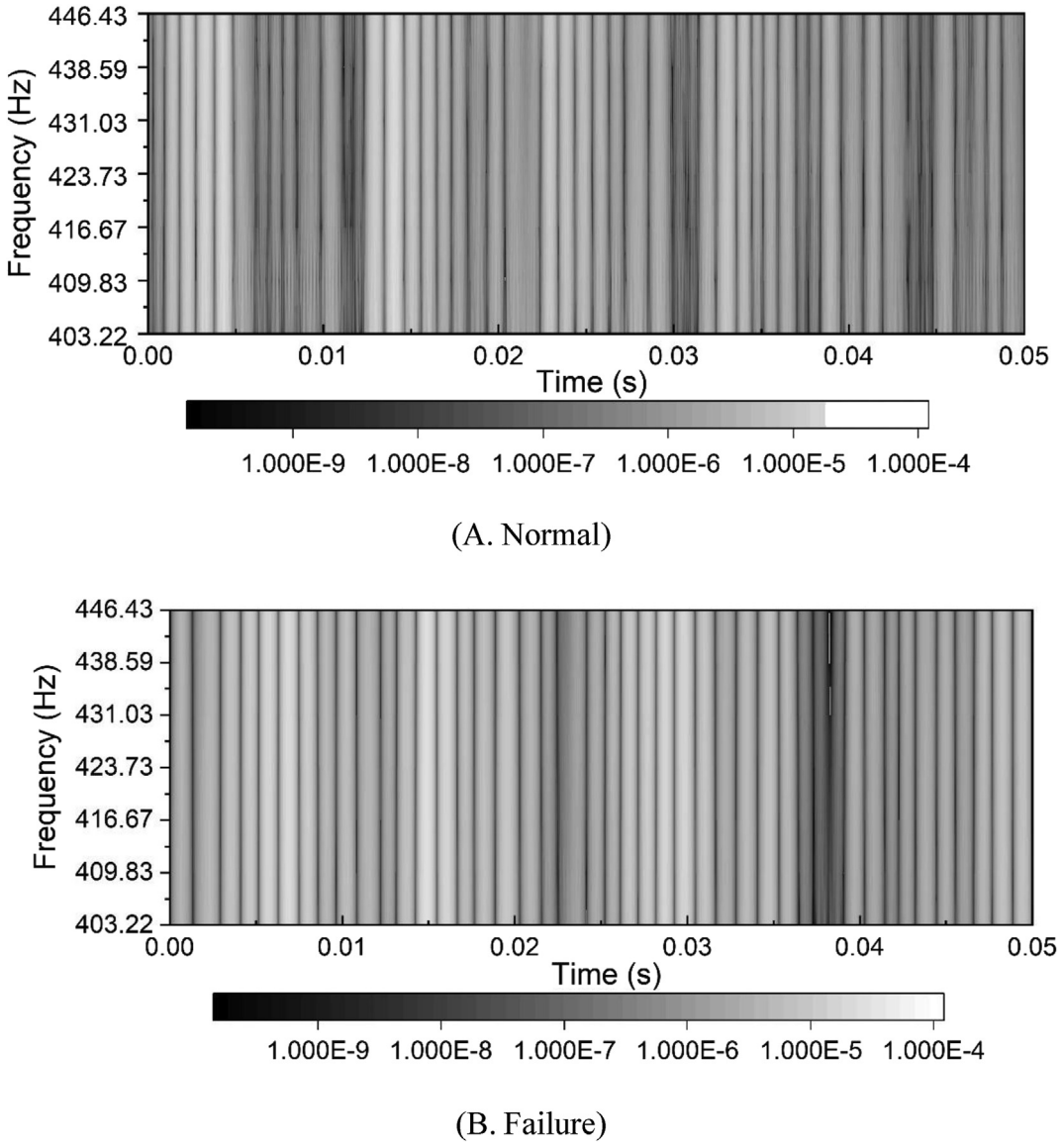

Fig. 9. Wavelet analysis results.

After the convolutional layer, max pooling layer, and activation function are worked several times, the data usually shift to one or more fully connected layers [14,33,34]. A fully connected layer is a one-dimensional array of numbers used for classification and is connected to all outputs [35]. Before classification, the data pass through the SoftMax layer to convert probability numbers into prediction numbers.

In our research, the bearing failure in an excavator motor was classified using a 1-D CNN; the time waveform was chosen as the input data. The CNN model structure is shown in Fig. 10.

Our CNN model consists of an input layer, two convolutional combinations (convolution, batch normalization, and ReLU), two max-pooling layers, three fully connected layers, a dropout layer, a SoftMax layer and a classification output. The layer types and specifications are presented in Table 2.

4. CNN results

In this study, the measured data were classified into normal and failure categories. Time-domain data were used for CNN training. The learning curve for the CNN is shown in Fig. 11. A total of 24,000 data points were used for CNN training; each data point represented one rotation of the motor. Ninety percent of the data was used for training and validation; 10% was used for testing.

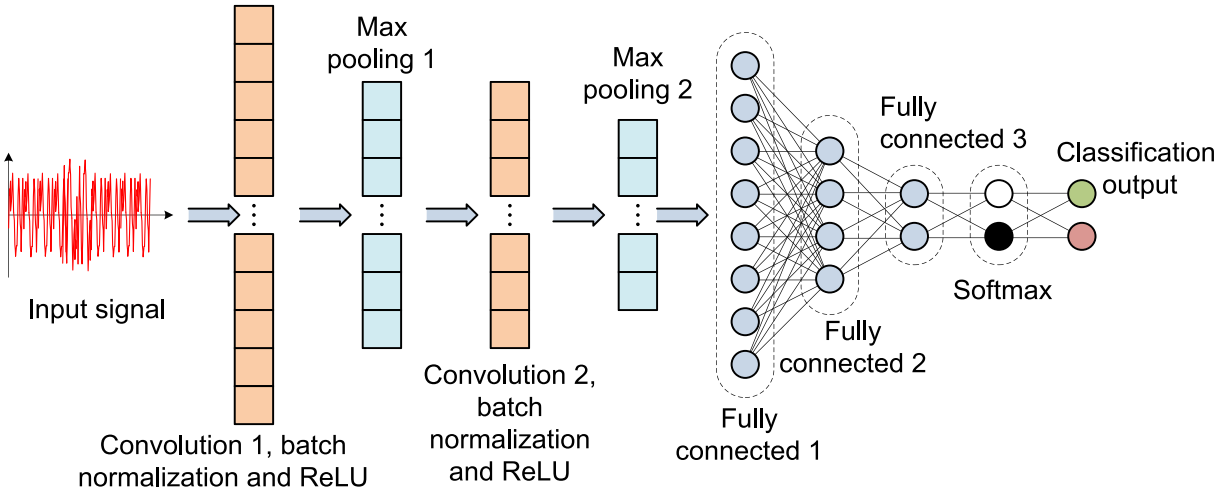

Fig. 10. Structure of 1-D CNN model for bearing failure prediction.

Table 2. Layers of 1-D CNN model for bearing failure prediction.

Layer name	Specification
Image input	$1 \times 5000 \times 1$ images with "zerocenter" normalization
Convolution	100 $1 \times 1024 \times 1$ convolutions with stride [22] and padding [0 0 0 0]
Batch normalization	Batch normalization with 100 channels
ReLU	ReLU
Max pooling	1×9 max pooling with stride [22] and padding [0 0 0 0]
Convolution	100 $1 \times 256 \times 100$ convolutions with stride [11] and padding [0 0 0 0]
Batch normalization	Batch normalization with 100 channels
ReLU	ReLU
Max pooling	1×9 max pooling with stride [22] and padding [0 0 0 0]
Fully connected	500 fully connected layers
Dropout	50% dropout
Fully connected	250 fully connected layers
Fully connected	2 fully connected layers in "CNN with 2 classifications" (eleven fully connected layers in "CNN with 11 classifications")
SoftMax	SoftMax
Classification output	Crossentropyex with classes "A (Normal)" and "B (Failure)" in the "CNN with 2 classifications" (A (Normal), B (Failure-10%), C (Failure-20%), D (Failure-30%), E (Failure-40%), F (Failure-50%), G (Failure-60%), H (Failure-70%), I (Failure-80%), J (Failure-90%), K (Failure) in "CNN with 11 classifications")

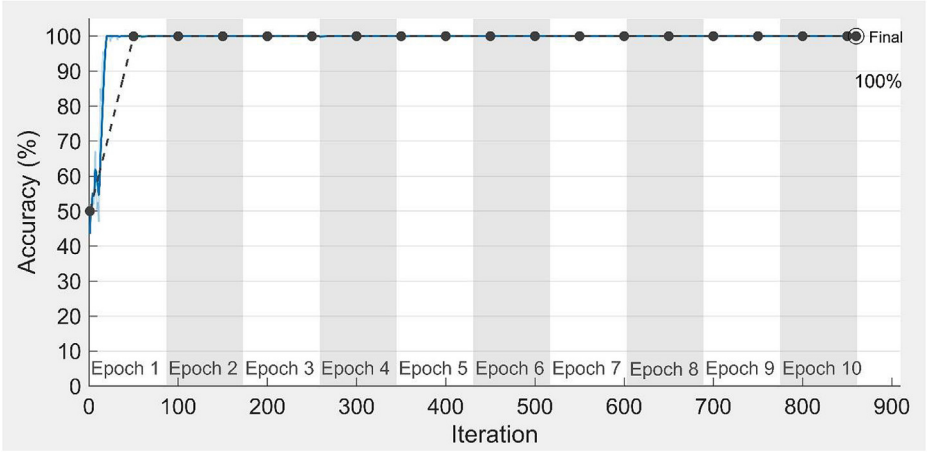

Fig. 11. Learning curve for "CNN with 2 classifications" [37].

Table 3. Learning specifications of "CNN with 2 classifications".

Epoch	Iteration	Time elapsed (hh:mm:ss)	Mini-batch accuracy	Validation accuracy	Mini-batch loss	Validation loss	Base learning rate
1	1	00:18:55	43.50%	50.00%	3.4946	7.9712	0.0010
2	150	00:32:13	100.00%	99.98%	1.9014e-07	0.0013	0.0010
3	250	00:40:34	100.00%	99.98%	2.4438e-07	0.0011	0.0010
4	300	00:44:45	100.00%	100.00%	8.8397e-07	2.6324e-06	0.0010
5	400	00:53:04	100.00%	100.00%	1.3292e-06	1.5160e-06	0.0010
6	500	01:01:22	100.00%	100.00%	2.3945e-06	1.4980e-06	0.0010
7	600	01:09:41	100.00%	100.00%	8.2674e-07	1.5154e-06	0.0010
8	650	01:13:57	100.00%	100.00%	1.4273e-05	1.5173e-06	0.0010
9	750	01:22:17	100.00%	100.00%	1.4842e-07	1.0371e-06	0.0010
10	860	01:32:10	100.00%	100.00%	1.8954e-07	1.0105e-06	0.0010

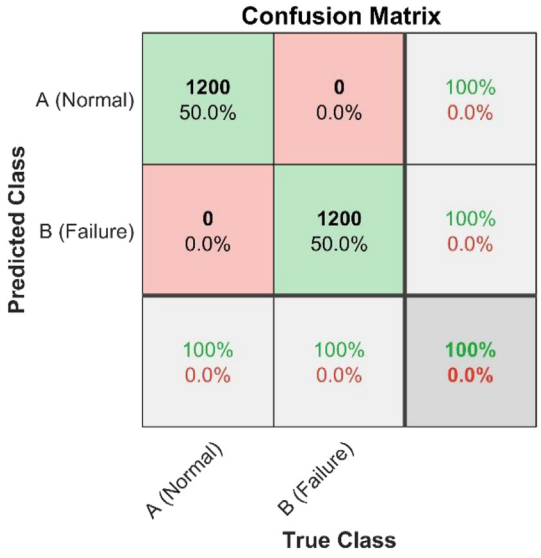

Fig. 12. Confusion matrix for "CNN with 2 classifications" [37].

In Fig. 11, the validation accuracy of CNN learning was evaluated as 100%. The CNN learning specifications are presented in Table 3.

Figure 12 shows the bearing health classification test accuracy results, known as a confusion matrix, showing predictions of randomly selected data (10% of total data). Randomly selected bearing data were classified into normal and failure categories.

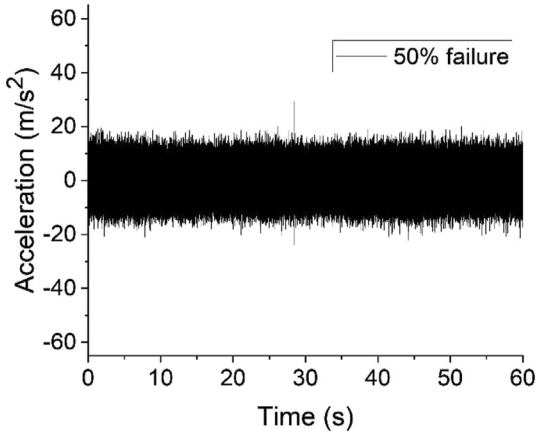

Fig. 14. 50% failure waveform.

The horizontal axis shows the actual bearing condition, and the vertical axis shows the test results of the trained CNN model. The test verifies the model training process. The diagonal of the matrix expresses the test accuracy of the trained "CNN with 2 classifications", visualized in green. In Fig. 12, the test accuracy is 100%. The confusion matrix result presents the CNN model prediction accuracy; the CNN can accurately assess the bearing health conditions.

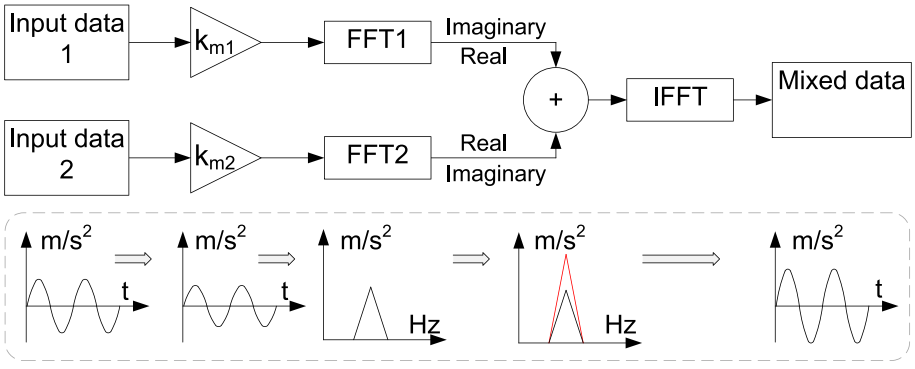

Fig. 13. Structure of data generation method.

In practice, the bearing health deterioration rate must be determined clearly and in detail to implement predictive maintenance. Normal and failure data alone are insufficient in determining the level of bearing health deterioration. New data must be created to represent different levels of motor-bearing health deterioration.

5. Verification of proposed system

New data generation is essential to create an accurate CNN model to assess bearing failure. New data were generated to represent motor-bearing health deterioration levels in increments of 10%. After creating these data, a new CNN model was trained to determine the motor-bearing health more accurately. The RUL of the bearing can be easily determined using the new CNN model. Data generation requires several signal processing techniques, including FFT, Inverse Fast Fourier Transform (IFFT), and combinations of both.

5.1. Test waveform preparation for verification

As previously observed, when bearing failure increases, the amplitude of the vibration is elevated

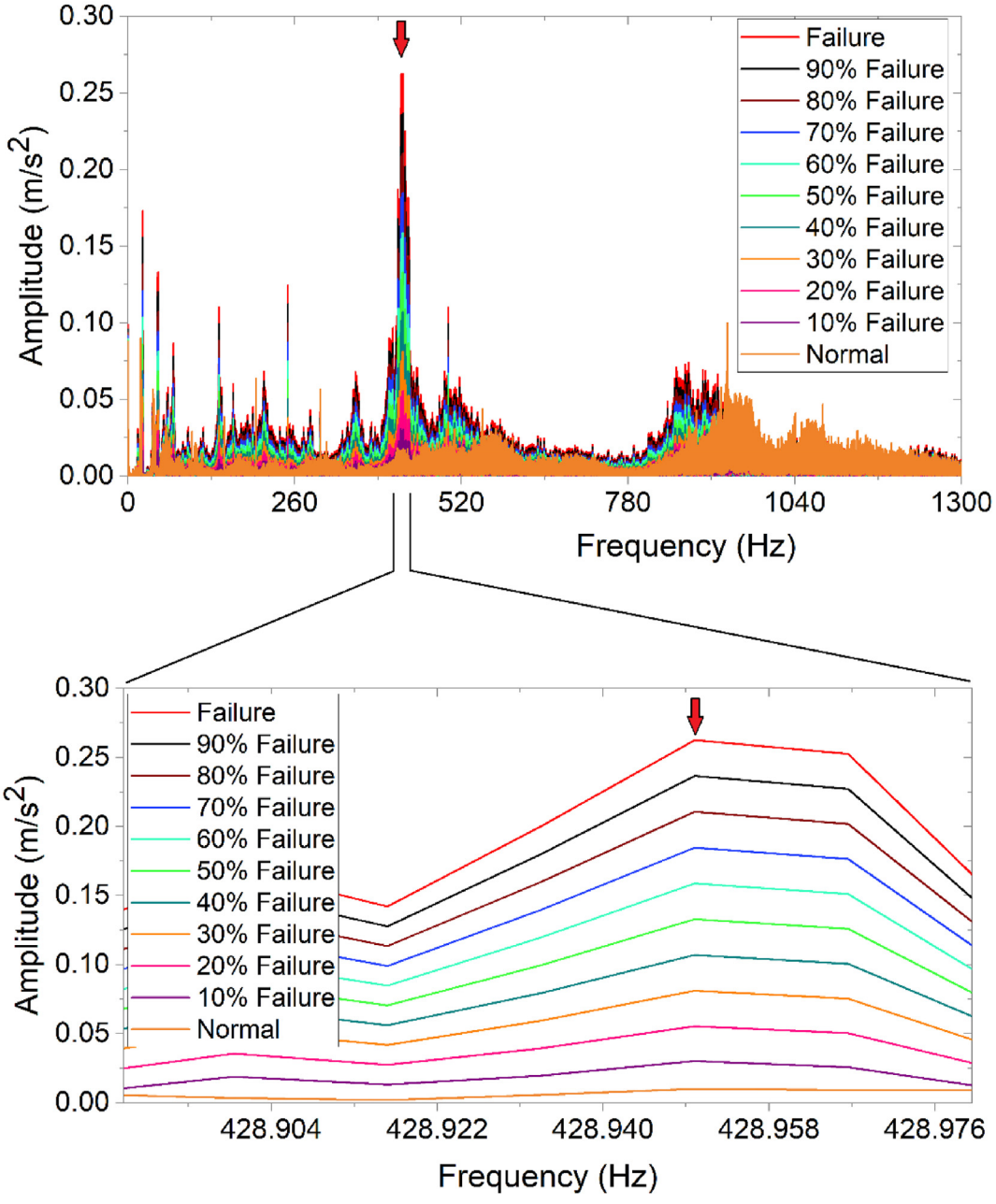

Fig. 15. FFT analysis results for all data.

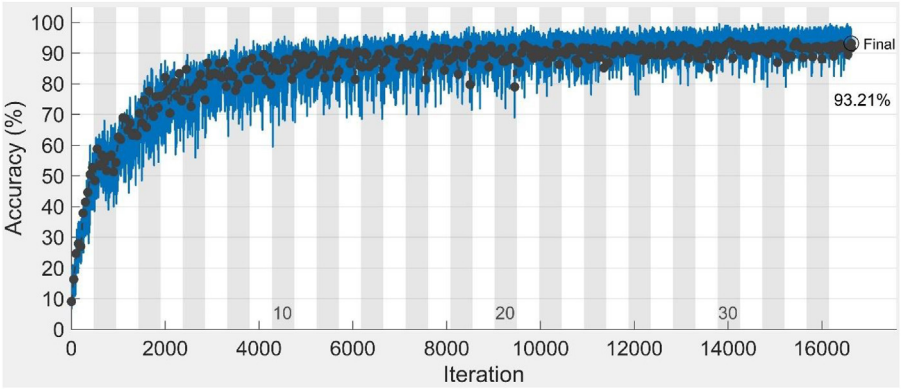

Fig. 16. Learning curve for "CNN with 11 classifications".

linearly in the same frequency range between 400 and 450 Hz. Therefore, bearing deterioration level amplitudes increase from normal to failure in this range. In order to generate data, the following actions are performed. Measured vibrations (normal and failure) should be converted to the frequency domain using FFT, and consequently, data is extracted for each frequency. Thereafter, one dataset is added to another to generate mixed data. In this case, normal should be added on failure. Before these actions, the normal and failure data should be multiplied by the mixing coefficient. The mixing coefficient can be from 0 to 1. For example, to generate 50% failure data, normal and failure data should be multiplied by 0.5, respectively. Or, to generate 40% failure data, normal should be multiplied by 0.6, and failure multiplied by 0.4. Thus, the data generating (mixing) process is performed until all necessary data has been generated. Also, data must be converted to complex numbers when using FFT. The real part of the normal data is added to the real part of the failure data. This action is repeated for the imaginary parts of the data. The generation is performed according to the schema named as the structure of the data generation new method (data mixing method), which is shown in Fig. 13, where k_m is the mixing coefficient. After that, the summed real and imaginary numbers were converted into time-domain data using IFFT to produce mixed data.

5.2. Inverse Fast Fourier Transform

Before generating new data, the frequency-domain data is converted to time-domain data using the Inverse Fast Fourier Transform (IFFT), particularly for the data mixing processes. IFFT is also an important technique for signal processing.

5.3. Generated waveform and verification

New data was created (mixed) from the normal and failure motor bearing data using the novel data generation method. The generated eleven levels of motor-bearing health deterioration data express gradual bearing health deterioration from normal to failure in increments of 10%. Figure 14 shows the 50% failure waveform, which is representative of all generated data.

The time-domain waveforms of the generated data were similar, as shown in Figs. 7 and 14. It was difficult to distinguish their differences. FFT analysis was performed on these data. The results for all data are plotted in Fig. 15; the differences are easily distinguished.

From FFT analysis, the dominant frequencies of motor bearing failure were determined to be between 400 Hz and 450 Hz, as shown in Fig. 15. In this region, the vibration amplitude of bearing failure gradually increases linearly, confirming that the data were correctly generated. The area indicated by the red arrow is enlarged to clearly show the linear increase. The frequency band from 800 to 1100 Hz is gradually shifting to the left, as shown in Fig. 15.

The data (generated and measured) were classified into 11 categories: normal, 10% failure, 20% failure, 30% failure, 40% failure, 50% failure, 60% failure, 70% failure, 80% failure, 90% failure and total failure. A total of 132,000 data points were used for CNN learning, each representing one rotation of the motor; each category contained 12,000 data points.

The learning curve for the "CNN with 11 classifications" is shown in Fig. 16. The CNN learning was complicated owing to a large amount of data and little difference between the data in the 11 categories. Thus, the maximum epoch number for CNN learning was increased to 35. The maximum epoch number

Table 4. Learning specifications of "CNN with 11 classifications".

Epoch	Iteration	Time elapsed (hh:mm:ss)	Mini-batch accuracy	Validation accuracy	Mini-batch loss	Validation loss	Base learning rate
1	1	00:19:05	6.50%	9.09%	6.9368	13.7760	0.0010
5	2350	06:45:12	84.00%	74.42%	0.5057	0.7599	0.0010
10	4750	13:18:14	87.00%	84.15%	0.4277	0.4696	0.0010
15	7100	19:32:52	89.00%	87.41%	0.2690	0.3405	0.0010
20	9500	25:59:22	94.00%	87.49%	0.2415	0.3654	0.0010
25	11850	32:18:46	94.50%	92.50%	0.1605	0.2118	0.0010
30	14250	38:49:00	93.00%	90.71%	0.2229	0.2850	0.0010
35	16625	45:17:50	94.50%	91.68%	0.1965	0.2750	0.0010

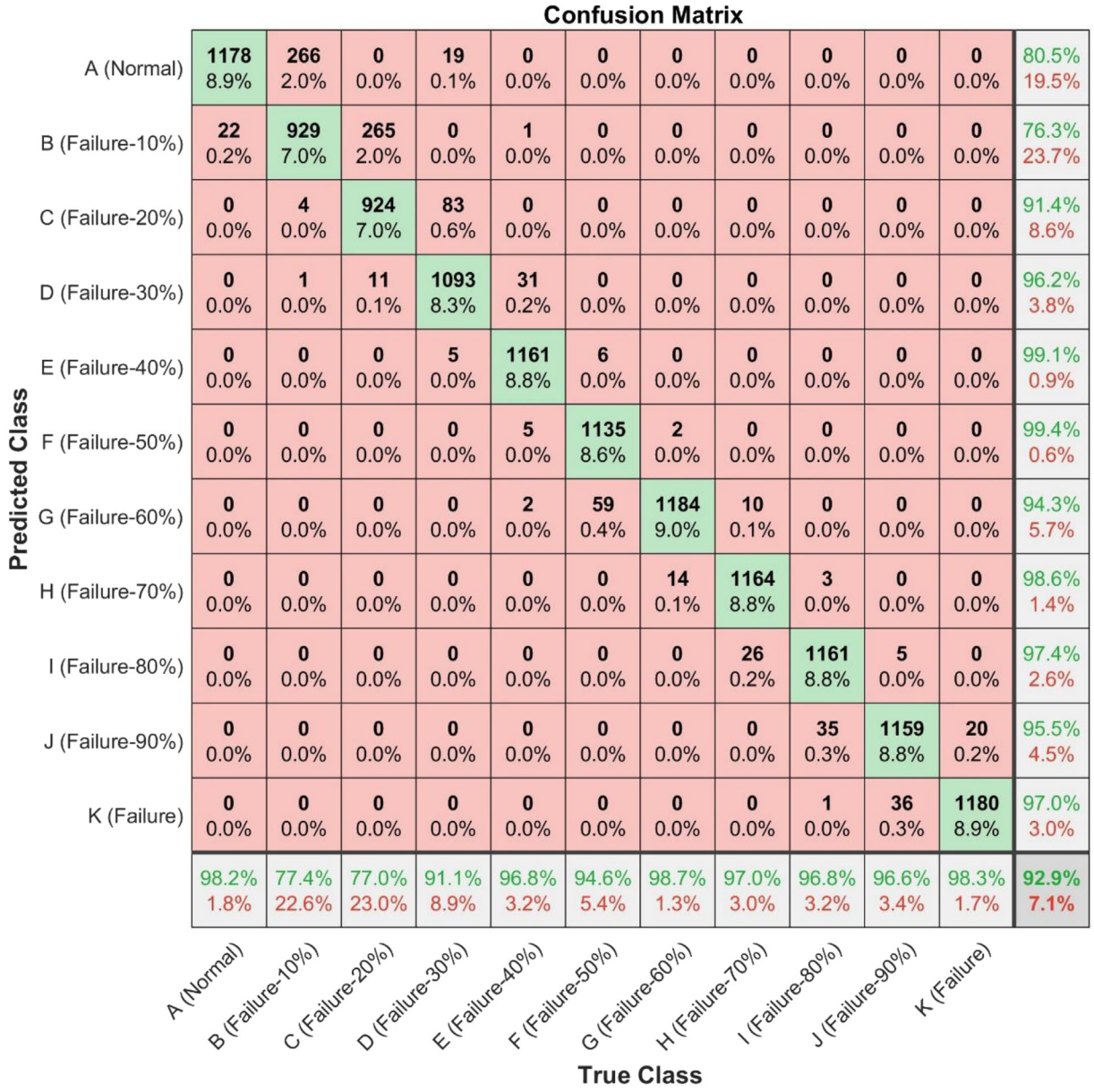

Fig. 17. Confusion matrix for "CNN with 11 classifications".

was 10 for training the "CNN with 2 classifications", as shown in Fig. 11. The validation accuracy reached 93.21%. The last learning process required more time than the "CNN with 2 classifications". The CNN learning specifications are presented in Table 4.

In Table 4, only a few max epoch numbers are presented for a clear description and to save page space. Figure 17 shows the test accuracy results for the "CNN with 11 classifications" in a confusion matrix and the predictions of randomly selected data (10% of total data). All randomly selected data were classified into 11 categories.

In Fig. 17, the overall test accuracy is 92.9%. The prediction (test) accuracy is over 90% for all categories except failure-10% and failure-20%, visualized diagonally in green. There were a total of 13,200 test data points; each category contained 9.09% of the total test data. If the CNN model prediction is assumed to have 100% accuracy, the predicted number for each category must be 1200. The test accuracy for the "CNN with 11 classifications" is 92.9%, which is an acceptable result. The confusion matrix result shows that the "CNN with 11 classifications" can assess bearing health deterioration levels with good accuracy. The "CNN with 11 classifications" confirms that data generation, FFT, and wavelet analysis were performed properly. As almost all of the data were predicted correctly, each category expresses unique features. Nearly all falsely predicted datasets were classified as neighbor categories, such as the 266 data values belonging to "Failure-10%" data misclassified as "Normal", 4 "Failure-10%" data as "Failure-20%", 265 "Failure-20%" data as "Failure-10%", 11 "Failure-20%" data as "Failure-30%", etc. This shows that neighbor categories have similar features, which in turn expresses the degree of the practicality of these generated datasets. Hence, all falsely classified data is located near the green diagonal of Fig. 17 confusion matrix.

5.4. Real-time bearing health monitoring

In an actual system, machine health monitoring requirements are imposed, including good diagnostics, inexpensive apparatus, simple operation, and low technical requirements. To satisfy these requirements, the machine monitoring system should be simple. Thus the "CNN with 2 classifications" was used instead of the "CNN with 11 classifications". The "CNN with 11 classifications" has high technical requirements that make it difficult to use in actual conditions. The price of diagnostic systems has also increased. For this reason, the "CNN with two classifications" was checked using all data (generated and measured) to represent motor bearing health deterioration levels in 10% increments.

To check the "CNN with 2 classifications", one-wave data collection was created, which is the unity of data that expresses 10% bearing health deterioration levels. The results of the one-wave data wavelet analysis determined whether the data collection was correct, as shown in Fig. 18.

The vibration amplitude in the dominant frequency band from 400 to 450 Hz gradually increased. The dark color represents low amplitude, and the light color represents high amplitude. The graph shows that the bearing vibration was normal at the initial time; the bearing vibration increased gradually until failure occurred, indicating that the one-wave data were created correctly.

The checking result for the simple CNN model is shown in Fig. 19.

Figure 19 shows how the simple bearing health monitoring system works. The simple CNN (CNN

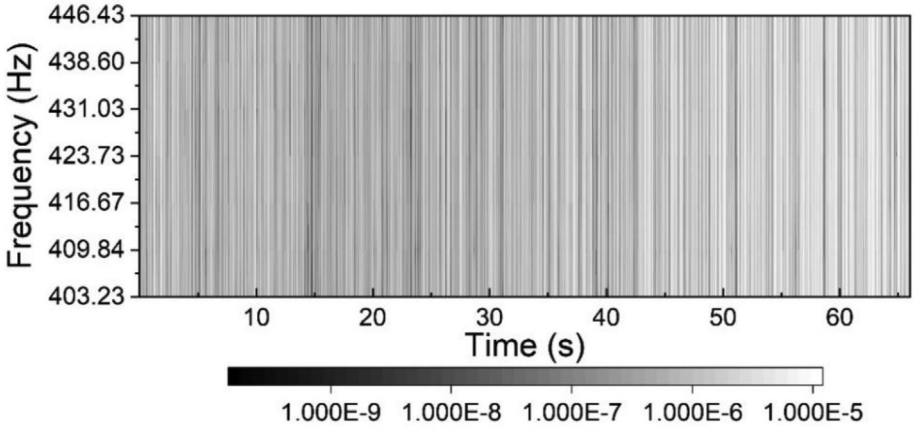

Fig. 18. Wavelet analysis of real-time bearing health deterioration.

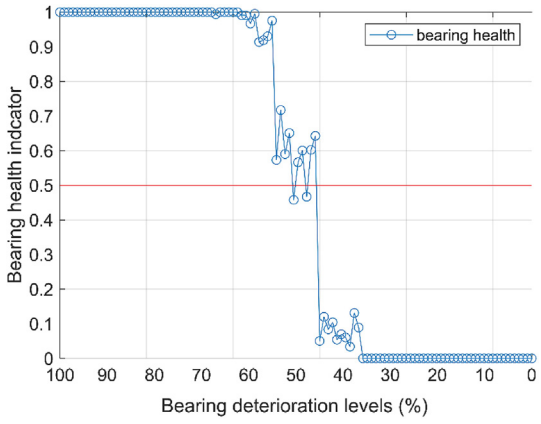

Fig. 19. Real-time bearing monitoring.

with 2 classifications) model can predict the bearing health deterioration levels in a general manner. A simple CNN model has two indicators of bearing health, normal and failure. The normal indicator on the vertical axis in Fig. 19 represents the average CNN prediction number; the horizontal axes represent the bearing health levels. When the simple CNN model is used for actual systems, the bearing health deterioration levels are predicted, as shown in Fig. 19. The simple CNN model can predict bearing health with sufficient accuracy; hence the RUL of the bearing would be determined using this model.

6. Conclusions

In this study, a vibration-based early diagnostic system using a CNN was proposed for mining excavator motor bearings. In the past, motor bearing failures were detected by experienced operators based on vibration. The diagnosis was not reliable due to human error. This study was conducted as a solution to this problem.

Two CNNs were trained in this study: a "CNN with 2 classifications" and a "CNN with 11 classifications". The prediction accuracy of the "CNN with 2 classifications" was 100%. FFT and wavelet analysis were performed; the dominant frequency range of bearing failure was determined to be from 400 to 450 Hz.

New data were generated to estimate the RUL of the bearing and observe its health deterioration. The generated (mixed) data represent bearing health deterioration increasing gradually in increments of 10%. All data (generated and measured) were used to train a new "CNN model with 11 classifications". The "CNN with 11 classifications" was successfully trained; the prediction accuracy was 92.9%.

A real-time bearing health monitoring graphic was obtained using one-wave data and the "CNN with 2 classifications". One-wave data were created based on all the data to represent the bearing health deterioration in increments of 10%. This monitoring system has advantages, including reduced diagnostic system cost, low technical requirements, and simple implementation.

Ethical statement

The authors state that the research was conducted according to ethical standards.

Funding body

This research was funded by the Japan Society for the Promotion of Science (JSPS) on the *Core-to-Core Program*. The project title is "Establishment of Research and Education Hub to Develop Young Researchers on Mining Informatics for Sustainable Resource Development in Middle Asian Countries", and the number is FY2021-5.

Conflict of interest

None declared.

Acknowledgements

We thank our labmates Rei Hosoda, Lesego Senjoba, Brian Bino Sinaice, Elsa Pansilvania Andre Manjate, Narihiro Owada and a friend Orkhon Lkhamjav for providing valuable advice and support.

References

[1] Introduction of the Baganuur mine. http://baganuurmine.mn/%D1%82%D0%B0%D0%BD%D0%B8%D0%BB%D1%86%D1%83%D1%83%D0%BB%D0%B3%D0%B0/ (accessed Nov. 02, 2021).

[2] Singh GK, Ahmed Saleh Al Kazzaz S. Induction machine drive condition monitoring and diagnostic research—a survey. Elec Power Syst Res Feb. 2003;64(2):145–58. https://doi.org/10.1016/S0378-7796(02)00172-4.

[3] He F, Xie G, Luo J. Electrical bearing failures in electric vehicles. Friction Feb. 2020;8(1):4–28. https://doi.org/10.1007/s40544-019-0356-5.

[4] Irfan M, Saad N, Ibrahim R, Asirvadam VS, Magzoub M, Hung NT. A non-invasive method for condition monitoring of induction motors operating under arbitrary loading conditions. Arabian J Sci Eng Sep. 2016;41(9):3463–71. https://doi.org/10.1007/s13369-015-1996-z.

[5] Zhang S, et al. Model-based analysis and quantification of bearing faults in induction machines. IEEE Trans Ind Appl May 2020;56(3):2158–70. https://doi.org/10.1109/TIA.2020.2979383.

[6] Ozcan IH, Devecioglu OC, Ince T, Eren L, Askar M. Enhanced bearing fault detection using multichannel, multilevel 1D CNN classifier. Electr Eng May 2021. https://doi.org/10.1007/s00202-021-01309-2.

[7] A guide to preventing failure. ABB; 2015. Accessed: Nov. 02, 2021. [Online]. Available: https://new.abb.com/docs/librariesprovider53/about-downloads/motors_ebook.pdf?sfvrsn=4.

[8] Shen C, Wang D, Kong F, Tse PW. Fault diagnosis of rotating machinery based on the statistical parameters of wavelet packet paving and a generic support vector regressive classifier. Measurement May 2013;46(4):1551–64. https://doi.org/10.1016/j.measurement.2012.12.011.

[9] Jia F, Lei Y, Lin J, Zhou X, Lu N. Deep neural networks: a promising tool for fault characteristic mining and intelligent diagnosis of rotating machinery with massive data. Mech Syst Signal Process May 2016;72(73):303–15. https://doi.org/10.1016/j.ymssp.2015.10.025.

[10] Li C, Sanchez R-V, Zurita G, Cerrada M, Cabrera D, Vásquez RE. Gearbox fault diagnosis based on deep random forest fusion of acoustic and vibratory signals. Mech Syst Signal Process Aug. 2016;76(77):283–93. https://doi.org/10.1016/j.ymssp.2016.02.007.

[11] Shao H, Jiang H, Zhang H, Duan W, Liang T, Wu S. Rolling bearing fault feature learning using improved convolutional deep belief network with compressed sensing. Mech Syst Signal Process Feb. 2018;100:743–65. https://doi.org/10.1016/j.ymssp.2017.08.002.

[12] Ince T, et al. Early bearing fault diagnosis of rotating machinery by 1D self-organized operational neural networks. IEEE Access 2021;9:139260–70. https://doi.org/10.1109/ACCESS.2021.3117603.

[13] Guan X, Chen G. Sharing pattern feature selection using multiple improved genetic algorithms and its application in bearing fault diagnosis. J Mech Sci Technol Jan. 2019;33(1):129–38. https://doi.org/10.1007/s12206-018-1213-6.

[14] Zhang X, Chen G, Hao T, He Z. Rolling bearing fault convolutional neural network diagnosis method based on casing signal. J Mech Sci Technol Jun. 2020;34(6):2307–16. https://doi.org/10.1007/s12206-020-0506-8.

[15] Eren L, Ince T, Kiranyaz S. A generic intelligent bearing fault diagnosis system using compact adaptive 1D CNN classifier. J Signal Process Syst Feb. 2019;91(2):179–89. https://doi.org/10.1007/s11265-018-1378-3.

[16] Chen C-C, Liu Z, Yang G, Wu C-C, Ye Q. An improved fault diagnosis using 1D-convolutional neural network model. Electronics Dec. 2020;10(1):59. https://doi.org/10.3390/electronics10010059.

[17] Wang D, Guo Q, Song Y, Gao S, Li Y. Application of multiscale learning neural network based on CNN in bearing fault diagnosis. J Signal Process Syst Oct. 2019;91(10):1205–17. https://doi.org/10.1007/s11265-019-01461-w.

[18] Chen X, Zhang B, Gao D. Bearing fault diagnosis base on multi-scale CNN and LSTM model. J Intell Manuf Apr. 2021;32(4):971–87. https://doi.org/10.1007/s10845-020-01600-2.

[19] Li G, Deng C, Wu J, Xu X, Shao X, Wang Y. Sensor data-driven bearing fault diagnosis based on deep convolutional neural networks and S-transform. Sensors Jun. 2019;19(12):2750. https://doi.org/10.3390/s19122750.

[20] Randall RB, Antoni J. Rolling element bearing diagnostics—a tutorial. Mech Syst Signal Process Feb. 2011;25(2):485–520. https://doi.org/10.1016/j.ymssp.2010.07.017.

[21] Ding Yunhao, Jia Minping. A multi-scale convolutional auto-encoder and its application in fault diagnosis of rolling bearings, vol. 35; 2019. p. 471. https://doi.org/10.3969/j.issn.1003-7985.2019.04.003. 423.

[22] Guo L, Lei Y, Xing S, Yan T, Li N. Deep convolutional transfer learning network: a new method for intelligent fault diagnosis of machines WithUnlabeled data. IEEE Trans Ind Electron Sep. 2019;66(9):7316–25. https://doi.org/10.1109/TIE.2018.2877090.

[23] Lei Y, Lin J, Zuo MJ, He Z. Condition monitoring and fault diagnosis of planetary gearboxes: a review. Measurement Feb. 2014;48:292–305. https://doi.org/10.1016/j.measurement.2013.11.012.

[24] Samanta B. Artificial neural networks and genetic algorithms for gear fault detection. Mech Syst Signal Process 2004;18(5):1273–1282, Sep. https://doi.org/10.1016/j.ymssp.2003.11.003.

[25] Bin GF, Gao JJ, Li XJ, Dhillon BS. Early fault diagnosis of rotating machinery based on wavelet packets—empirical mode decomposition feature extraction and neural network. Mech Syst Signal Process Feb. 2012;27:696–711. https://doi.org/10.1016/j.ymssp.2011.08.002.

[26] Wang Y, Yang C, Xu D, Ge J, Cui W. Evaluation and prediction method of rolling bearing performance degradation based on attention-LSTM. Shock Vib May 2021;2021:1–15. https://doi.org/10.1155/2021/6615920.

[27] Senjoba L, Sasaki J, Kosugi Y, Toriya H, Hisada M, Kawamura Y. One-dimensional convolutional neural network for drill bit failure detection in rotary percussion drilling. Mining Nov. 2021;1(3):297–314. https://doi.org/10.3390/mining1030019.

[28] Schmidhuber J. Deep learning in neural networks: an overview. Neural Network Jan. 2015;61:85–117. https://doi.org/10.1016/j.neunet.2014.09.003.

[29] He Y, Gu C, Chen Z, Han X. Integrated predictive maintenance strategy for manufacturing systems by combining quality control and mission reliability analysis. Int J Prod Res Oct. 2017;55(19):5841–62. https://doi.org/10.1080/00207543.2017.1346843.

[30] Sullivan GP, Pugh R, Melendez AP, Hunt WD. Operations & maintenance best practices: guide to achieving operational efficiency. 2010 [Online]. Available: https://www.energy.gov/sites/prod/files/2013/10/f3/omguide_complete.pdf.

[31] Tran Anh D, Dąbrowski K, Skrzypek K. The predictive maintenance concept in the maintenance department of the 'industry 4.0' production enterprise. Found Manag Dec. 2018;10(1):283–92. https://doi.org/10.2478/fman-2018-0022.

[32] Najmi A-H, Sadowsky J. The continuous wavelet transform and variable resolution time–frequency analysis. Johns Hopkins APL Tech Dig 1997;18(1):8.

[33] Sinaice BB, Kawamura Y, Kim J, Okada N, Kitahara I, Jang H. Application of deep learning approaches in igneous rock hyperspectral imaging. In: Topal E, editor. Proceedings of the 28th international symposium on mine planning and equipment selection - MPES 2019. Cham: Springer International Publishing; 2020. p. 228–35. https://doi.org/10.1007/978-3-030-33954-8_29.

[34] Okada N, Maekawa Y, Owada N, Haga K, Shibayama A, Kawamura Y. Automated identification of mineral types and grain size using hyperspectral imaging and deep learning for mineral processing. Minerals Sep. 2020;10(9):809. https://doi.org/10.3390/min10090809.

[35] Yamashita R, Nishio M, Do RKG, Togashi K. Convolutional neural networks: an overview and application in radiology. Insights Imag Aug. 2018;9(4):611–29. https://doi.org/10.1007/s13244-018-0639-9.

[36] Sharma S, Sharma S, Scholar U, Athaiya A. Activation functions in neural networks. Int J Eng Appl Sci Technol 2020;4(12):310–6. ISSN No. 2455-2143.

[37] Annual Report 2020.4 - 2021.3. Center for regional revitalization in research and education, akita university [Online]. Available: https://www.akita-u.ac.jp/honbu/social/pdf/r2_nenpou.pdf.

[38] Ma L, Ding Y, Wang Z, Wang C, Ma J, Lu C. An interpretable data augmentation scheme for machine fault diagnosis based on a sparsity-constrained generative adversarial network. Expert Syst Appl Nov. 2021;182:115234. https://doi.org/10.1016/j.eswa.2021.115234.

[39] Bui V, Pham TL, Nguyen H, Jang YM. Data augmentation using generative adversarial network for automatic machine fault detection based on vibration signals. Appl Sci Mar. 2021;11(5):2166. https://doi.org/10.3390/app11052166.

[40] Pan T, Chen J, Zhang T, Liu S, He S, Lv H. Generative adversarial network in mechanical fault diagnosis under small sample: a systematic review on applications and future

perspectives. ISA Trans Sep. 2022;128:1–10. https://doi.org/10.1016/j.isatra.2021.11.040.
[41] Zhao B, Yuan Q. Improved generative adversarial network for vibration-based fault diagnosis with imbalanced data. Measurement Feb. 2021;169:108522. https://doi.org/10.1016/j.measurement.2020.108522.
[42] Guo Q, Li Y, Song Y, Wang D, Chen W. Intelligent Fault diagnosis method based on full 1-D convolutional generative adversarial network. IEEE Trans Ind Inf Mar. 2020;16(3):2044–53. https://doi.org/10.1109/TII.2019.2934901.
[43] Song Y, Li Y, Jia L, Qiu M. Retraining strategy-based domain adaption network for intelligent fault diagnosis. IEEE Trans Ind Inf Sep. 2020;16(9):6163–71. https://doi.org/10.1109/TII.2019.2950667.
[44] Xia M, Li T, Shu T, Wan J, de Silva CW, Wang Z. A two-stage approach for the remaining useful life prediction of bearings using deep neural networks. IEEE Trans Ind Inf Jun. 2019;15(6):3703–11. https://doi.org/10.1109/TII.2018.2868687.
[45] Ren L, Sun Y, Cui J, Zhang L. Bearing remaining useful life prediction based on deep autoencoder and deep neural networks. J Manuf Syst Jul. 2018;48:71–7. https://doi.org/10.1016/j.jmsy.2018.04.008.
[46] Li X, Zhang W, Ding Q. Deep learning-based remaining useful life estimation of bearings using multi-scale feature extraction. Reliab Eng Syst Saf Feb. 2019;182:208–18. https://doi.org/10.1016/j.ress.2018.11.011.
[47] Mao W, He J, Tang J, Li Y. Predicting remaining useful life of rolling bearings based on deep feature representation and long short-term memory neural network. Adv Mech Eng Dec. 2018;10(12). https://doi.org/10.1177/1687814018817184.168781401881718.
[48] Nie L, Zhang L, Xu S, Cai W, Yang H. Remaining useful life prediction for rolling bearings based on similarity feature fusion and convolutional neural network. J Braz Soc Mech Sci Eng Aug. 2022;44(8):328. https://doi.org/10.1007/s40430-022-03638-0.
[49] Yang J, Peng Y, Xie J, Wang P. Remaining useful life prediction method for bearings based on LSTM with uncertainty quantification. Sensors Jun. 2022;22(12):4549. https://doi.org/10.3390/s22124549.
[50] Ge Y, Liu JJ, Ma JX. Remaining useful life prediction using deep multi-scale convolution neural networks. IOP Conf Ser Mater Sci Eng Jan. 2021;1043(3):32011. https://doi.org/10.1088/1757-899X/1043/3/032011.
[51] Wang C, Jiang W, Yang X, Zhang S. RUL prediction of rolling bearings based on a DCAE and CNN. Appl Sci Dec. 2021;11(23):11516. https://doi.org/10.3390/app112311516.